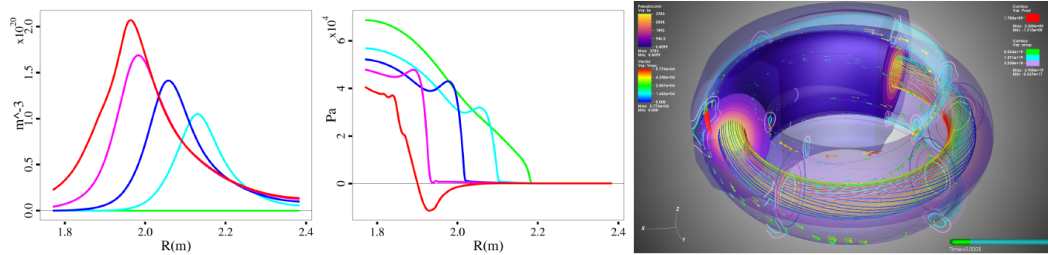


# Simulations and Validation of Disruption Mitigation and Projections to ITER's Disruption Mitigation System

Wednesday, May 12, 2021 12:10 PM (20 minutes)



Radial profiles of impurity density and pressure at  $t=[0.0,1.0,1.5,2.0,2.1]$ ms shows a persistent pressure bump as the impurities penetrate. 3D visualization at  $t=0.5$ ms shows flux aligned elongated spreading of impurities due to parallel flow driven by the pressure bump. ([click animation link for detailed description](#))

Figure 1: Impurity Density and Total Pressure Profiles and 3D Visualization

The efficacy of ITER's DMS must be evaluated within the next several years and, since in-situ evaluation is impossible, verified and validated simulations are critical. High fidelity 3D initial value simulations of Shattered Pellet Injection and Dispersive Shell Pellet (SPI and DSP) simulations show favorable verification and validation in cross code comparisons and comparisons to experiment. These successes develop the necessary confidence in their predictive capabilities of the Disruption Mitigation System (DMS) in ITER. Furthermore, simulations allow a flexible test bed to optimize and refine existing strategies and to develop new ones. To perform these critical 3D nonlinear initial value simulations we have implemented a particle based SPI and DSP model in the NIMROD code coupled to the single fluid resistive MHD equations modified with impurities and radiation[Vizzo2006].

	$\tau_{TQ}^S$	$\tau_{TQ}^E$	radfrac <sup>S</sup>	radfrac <sup>E</sup>
pure Ne	2.2 ms	1.7 ms	83%	89%
D2=10xNe	2.8 ms	2.3 ms	86%	75%
pure D2	5.6 ms	6.2 ms	4%	50%

Comparison of thermal quench time and radiated fraction for NIMROD(S) and DIII-D(E).

Figure 2: Comparison of NIMROD and DIII-D

The table summarizes the favorable comparison of NIMROD SPI simulations of the impurity scan to the DIII-D experiments[CCKim2019]. Both thermal quench times and radiated fractions show good agreement and the same trends. Comparisons of benchmark cases using a stationary, axisymmetric, on-axis source to the M3D-C1 results[BLyons2019] show very good agreement. Complementary efforts by the 3D MHD code MARS and Fokker-Planck code CQL3D demonstrate progress on modeling runaway electrons (RE) and the current quench. Dispersive Shell Pellets have demonstrated the advantage of an "inside-out" thermal quench where the central core temperature drops first and heat flux is subsequently inward. DSP modeling also shows potential advantages for RE loss and radiated energy fraction.

**SPI simulations** show that the ablating fragment drives strong parallel flows that transport the impurities along flux tubes and govern the thermal quench evolution. This parallel flow, caused by excess pressure (see figure) from ablation, is halted when the "head bites the tail", limiting the overall spreading of impurities,

and accounting for the observed radiation asymmetry peaking near the injector. SPI simulations also show that as the thermal quench proceeds, the peak radiation lags behind the ablating fragment and peaks in the accumulated cold impurities that builds up in the wake of the fragment trajectory. Impurity scans of mixed **deuterium/neon SPI pellets** show a more benign thermal quench due to the enhanced transport and dilution cooling caused by the addition of deuterium suggesting optimal pellet mixtures exist. Multi-injector SPI simulations demonstrate significant suppression of the  $n=1$  mode, the usual culprit for late thermal quench instabilities depicted in the figure at  $t=1.6\text{ms}$ . Symmetric **dual-injector** and **tri-injector** simulations show that suppressing the  $n=1$  instability results in a significantly more benign thermal quench with reduced radiation asymmetry and greater radiation fraction. The observations from these simulations, greatly assisted by 3D visualization tools and animations of the nonlinear evolving fields, are exploited and synthesized and tested in additional scenarios combining multiple injectors, different mixture pellets, and the addition of Massive Gas Injection to reduce the radiation asymmetry and overall heat loads. The most promising will be submitted for experiments on DIII-D and other tokamaks.

DSP simulations of the pre-thermal quench (TQ) phase indicate that a non-perturbative shell is achievable at quantities similar to the DIII-D experimental shell mass, which is the key to the high radiated energy fraction associated with DSP. Simulations carried through the end of the TQ show large amplitude MHD fluctuations ( $\delta B/B > 10^{-2}$ ) at the time of the plasma current spike—associated with current profile redistribution—which destroys all confinement by stochastizing fields and reducing field line connection lengths by at least three orders of magnitude. After the plasma current spike, which is of comparable amplitude to that measured in DIII-D experiments, no runaway electron tracer-particles remain confined. This result suggests that inside-out cooling may be particularly favorable to runaway electron de-confinement during the TQ, which is an unanticipated benefit of the concept. A large amplitude current spike is also observed in the stationary, axisymmetric, on-axis source benchmark cases with M3D-C1.

The generation and acceleration of runaway electrons poses an even greater uncertainty and threat than mitigation of the thermal load. Initial one-way coupling of time evolved thermal quench NIMROD fields to CQL3D demonstrates the sensitivity of runaway electron evolution to details of the thermal quench [RWHarvey2019]. These CQL3D-NIMROD simulations demonstrate that knock-on sources become more important in cases of slower, more realistic thermal quench. MARS-F modeling [YLiu2019] shows mitigation of a post-disruption, high-current runaway beam in DIII-D, due to the 1 kG level of magnetic field perturbation produced by a fast growing  $n = 1$  resistive kink instability. The RE loss is shown to be independent of the particle energy or the initial location of particles in the configuration space. Distributions of the lost REs to the DIII-D limiter surface show poloidally peaked profile near the high-field-side of the torus. Higher perturbation field level and/or higher particle energy also result in REs being lost to the low-field-side of the limiter surface. These complementary simulations will be used to compare and test a particle-in-cell runaway electron model implemented in NIMROD based on the hybrid kinetic-MHD energetic ion model. Ultimately, this hybrid kinetic-MHD RE model will provide comprehensive predictive 3D initial value simulations of the entire disruption mitigation scenario: from disruption trigger to thermal quench mitigation to current quench and runaway electron generation and mitigation, involving multiple injections and different strategies.

NIMROD DMS simulations of the  $Q=10$  ITER baseline scenario show that many of the same characteristics are seen in ITER thermal quenches as those observed in DIII-D, particularly the dominance of an  $n=1$  instability in the final thermal collapse. These simulations will be compared along side DIII-D and other (e.g. JET and KSTAR) tokamak DMS simulations and an initial assessment of the viability of the proposed DMS in ITER will be made.

*This material is based upon work supported by US DOE-OFES, under Awards DE SC0018109 - Center for Tokamak Transient Simulations, DE-SC0016452 - SCREAM, DE-FG02-95ER54309 - Fusion Theory, DE-FC02-04ER54698 - DIII-D, and GA ITER Contract ITER/CT/14/4300001108.*

## Affiliation

SLS2 Consulting/General Atomics

## Country or International Organization

United States

**Primary authors:** KIM, Charlson C. (SLS2 Consulting/General Atomics); IZZO, Valerie A. (Fiat Lux/General Atomics); HARVEY, R. W. (Bob) (CompX); PETROV, Yuri (CompX); LIU, Yueqiang (General Atomics); LYONS, Brendan (General Atomics); MCCLENAGHAN, Joseph (General Atomics)

**Co-authors:** PARKS, Paul (General Atomics); LAO, Lang (General Atomics); LEHNEN, Michael (ITER Organization); LOARTE, Alberto (ITER Organization)

**Presenter:** KIM, Charlson C. (SLS2 Consulting/General Atomics)

**Session Classification:** P3 Posters 3

**Track Classification:** Magnetic Fusion Theory and Modelling